

How unequal fluxes of high energy astrophysical neutrinos and antineutrinos can fake new physics

Hiroshi Nunokawa,^a Boris Panes^b and Renata Zukanovich Funchal^b

^aDepartamento de Física, Pontifícia Universidade Católica do Rio de Janeiro,
C.P. 38071, 22452-970, Rio de Janeiro, Brazil

^bInstituto de Física, Universidade de São Paulo,
C.P. 66.318, 05315-970 São Paulo, Brazil

E-mail: nunokawa@puc-rio.br, bapanes@if.usp.br, zukanov@if.usp.br

Received May 9, 2016

Revised August 31, 2016

Accepted October 4, 2016

Published October 21, 2016

Abstract. Flavor ratios of very high energy astrophysical neutrinos, which can be studied at the Earth by a neutrino telescope such as IceCube, can serve to diagnose their production mechanism at the astrophysical source. The flavor ratios for neutrinos and antineutrinos can be quite different as we do not know how they are produced in the astrophysical environment. Due to this uncertainty the neutrino and antineutrino flavor ratios at the Earth also could be quite different. Nonetheless, it is generally assumed that flavor ratios for neutrinos and antineutrinos are the same at the Earth, in fitting the high energy astrophysical neutrino data. This is a reasonable assumption for the limited statistics for the data we currently have. However, in the future the fit must be performed allowing for a possible discrepancy in these two fractions in order to be able to disentangle different production mechanisms at the source from new physics in the neutrino sector. To reinforce this issue, in this work we show that a wrong assumption about the distribution of neutrino flavor ratios at the Earth may indeed lead to misleading interpretations of IceCube results.

Keywords: neutrino astronomy, neutrino properties, cosmological neutrinos, neutrino detectors

ArXiv ePrint: [1604.08595](https://arxiv.org/abs/1604.08595)



Contents

1	Introduction	1
2	Neutrino and antineutrino production mechanisms and propagation	3
2.1	pp production	3
2.2	$p\gamma$ production	4
2.3	Effect of oscillation	4
3	On the interpretation of IceCube data	5
3.1	A possible scenario fitted with the wrong assumption	6
3.2	Re-thinking current results	8
4	Discussions and conclusions	10
A	Binned likelihood	12
B	Astrophysical neutrinos	12
C	High-energy neutrino background	13

1 Introduction

The discovery by the IceCube Collaboration that the Earth is bombarded by a flux of very high energy extraterrestrial neutrinos [1–3], opened a new research field, High Energy Neutrino Astronomy. Naturally, after these findings a big amount of activity has been devoted to studies about the origin of these neutrinos, see for instance [4–11]. Furthermore, as more data is collected it also becomes possible to study finer details about the observed neutrinos, which has motivated many studies devoted to address the flavor composition of this flux [12–19]. The reason to focus on composition studies relies on the fact that neutrino flavor composition can be used to tackle the production mechanism of very high energy neutrinos at the source, as well as to shed light on the possible presence of non-standard neutrino properties beyond the standard three flavor mixing scheme.

Understanding this process is utterly momentous as the same mechanism is expected to be at the genesis of very-high energy cosmic rays and photons [20–37]. We hope correlations among these ultra-high energy cosmic particles can be established in the near future helping us to unravel this long standing mystery. In the most frequently considered scenario, the decay of pions and subsequently of muons dominate the neutrino flux, producing the flux flavor ratios $(f_{\nu_e}^S : f_{\nu_\mu}^S : f_{\nu_\tau}^S)^1 = (\frac{1}{3} : \frac{2}{3} : 0)_S$ at the source [38]. However, the flux flavor composition at the source may vary from $(1 : 0 : 0)_S$ to $(0 : 1 : 0)_S$ under a profusion

¹Notice that here we are using italic f for the fractions. This is the notation that we use when we consider equal fractions of neutrinos and antineutrinos. Later, we will introduce a notation where fractions are specified with a normal f , in order to consider neutrinos and antineutrinos independently.

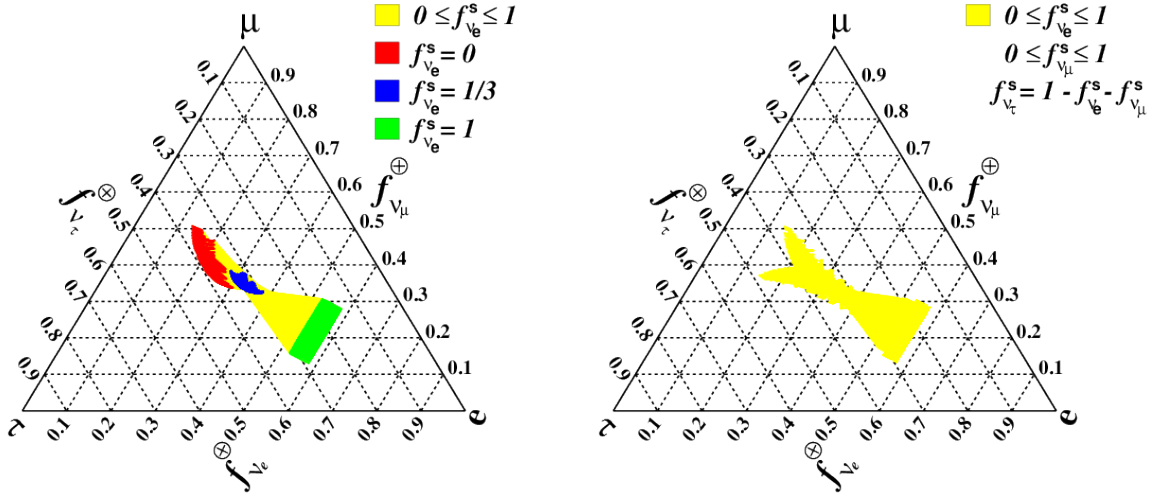


Figure 1. Currently allowed (expected) regions for the flux flavor ratios ($f_{\nu_e}^\oplus, f_{\nu_\mu}^\oplus, f_{\nu_\tau}^\oplus$) at the Earth by various high energy neutrino production scenarios denoted by the values of the parameter $f_{\nu_e}^S$ which lies somewhere between 0 and 1. On the left panel ν_τ are not allowed to be produced at the source, while on the right panel they are. We let neutrino mixing parameters vary within the current 3σ allowed regions [45]. Red, blue and green regions correspond to the case where $f_{\nu_e}^S = 0, 1/3$ and 1, respectively, whereas in the yellow regions, any value of $f_{\nu_e}^S \in [0, 1]$ is allowed.

of different scenarios which include muon energy loss [39–42], muon acceleration [43], and neutron decay [44].

After propagating over astronomical distances, as first pointed out by the authors of ref. [38], neutrino oscillations tend to equalize the flux flavor ratios to $(f_{\nu_e}^\oplus : f_{\nu_\mu}^\oplus : f_{\nu_\tau}^\oplus) \approx (\frac{1}{3} : \frac{1}{3} : \frac{1}{3})_\oplus$ at the Earth, for the expected source composition $(\frac{1}{3} : \frac{2}{3} : 0)_S$. In fact, by varying the neutrino oscillation mixing parameters in the regions allowed by the latest global fit [45] and by assuming any possible source flavor composition, it can be shown that the prediction for the flux flavor ratios at the Earth always end-up somewhere around the central point $(\frac{1}{3} : \frac{1}{3} : \frac{1}{3})_\oplus$, i.e., in a restricted region around the middle of the flavor-ratio triangle as can be seen on the left panel of figure 1 (see also [13, 46]). This remains true even if one allows for an arbitrary ν_τ content at the source, as depicted on the right panel of figure 1, although one predicts ν_τ contribution to be quite negligible [47].

Because of the limited variation of the neutrino flavor ratios at the Earth, some authors have speculated that a deviation of the neutrino flux flavor ratios from this central region of the flavor-ratio triangle could be interpreted as an indication of new physics at play in the neutrino sector. Among the other exotic possibilities, neutrino decay [48, 49], pseudo-Dirac neutrinos [50, 51], sterile neutrinos [52], Lorentz or CPT violation [53], quantum decoherence [54, 55], the impact of effective operators [46], non-standard neutrino interactions with dark matter [56], and so on, have been considered in the literature.

Moreover, although still statistically insignificant at the moment, fits to the IceCube data seem to be favoring flavor ratios at the Earth outside the allowed regions shown in figure 1, close to the edges of the flavor-ratio triangle [18, 57] that might signal a conflict with the standard expectation. If this is confirmed by future data, can this be an unambiguous sign of new physics or can this be explained by standard physics?

We show in this paper that in order to use neutrino flux flavor ratios at the Earth to probe the various production mechanism scenarios at the source, one cannot assume that neutrinos and antineutrinos fluxes at the Earth are the same when fitting the data. In particular, this assumption may lead to erroneous interpretation of the data in the future, and may already be the reason why the present best fit point for the flux flavor ratios seems to be outside the expected region.

In section 2 we briefly review the main high energy neutrino/antineutrino production mechanisms at astrophysical sources as well as the neutrino oscillation effect on their propagation to the Earth. In section 3 we discuss how unequal neutrino and antineutrino fluxes can affect the fitting of the shower and track events measured by IceCube. In particular, the fit of IceCube data by imposing the equality of neutrino and antineutrino flavor ratios at the Earth, when they are predicted to be not equal at the source and therefore at the Earth also, can produce allowed regions in the flavor-ratio triangle that lay outside the one expected by standard oscillation and consequently be misinterpreted as a sign of new physics. Finally, in section 4 we provide some discussions and our conclusions.

2 Neutrino and antineutrino production mechanisms and propagation

We do not know where or how exactly very high energy ($\gtrsim 100$ TeV) astrophysical neutrinos are produced. It is generally believed that their production takes place in transient astrophysical cosmic ray engines such as blazars (jets in active galactic nuclei) and gamma-ray bursts. The general idea behind the main mechanisms is that protons are accelerated and possibly confined in these sources by magnetic fields. The production of neutrons and charged pions and their succeeding decays produce neutrinos as well as other cosmic ray particles. Neutrinos, in particular, are produced via $\pi^+ \rightarrow \mu^+ \nu_\mu \rightarrow e^+ \nu_e \bar{\nu}_\mu \nu_\mu$ (and its charge conjugate process).

Depending on source properties such as the relative ambient gas and photon densities, pion production proceeds either by inelastic pp scattering [44] or by photo disintegration, primarily through the resonant processes $p\gamma \rightarrow \Delta^+ \rightarrow n\pi^+$, $p\pi^0$ [21].

2.1 pp production

If inelastic pp collisions are the dominant process of pion production, isospin invariance yields approximately equal numbers of π^\pm . Their decay followed by the decay of μ^\pm will lead to the flux flavor ratios at the source of

$$(f_{\nu_e}^S : f_{\nu_\mu}^S : f_{\nu_\tau}^S) \simeq (f_{\bar{\nu}_e}^S : f_{\bar{\nu}_\mu}^S : f_{\bar{\nu}_\tau}^S) \simeq \left(\frac{1}{6} : \frac{2}{6} : 0 \right)_S, \quad (2.1)$$

for both neutrinos and antineutrinos (note that sum of all fractions is normalized to 1).

Since in this case the flavor ratios are the same for neutrinos and antineutrinos, one can simply talk about the combined (neutrino+antineutrino) flavor ratios

$$\begin{aligned} (f_{\nu_e}^S : f_{\nu_\mu}^S : f_{\nu_\tau}^S) &\equiv (f_{\nu_e}^S + f_{\bar{\nu}_e}^S : f_{\nu_\mu}^S + f_{\bar{\nu}_\mu}^S : f_{\nu_\tau}^S + f_{\bar{\nu}_\tau}^S) \\ &= 2(f_{\nu_e}^S : f_{\nu_\mu}^S : f_{\nu_\tau}^S) = 2(f_{\bar{\nu}_e}^S : f_{\bar{\nu}_\mu}^S : f_{\bar{\nu}_\tau}^S) \\ &\simeq \left(\frac{1}{3} : \frac{2}{3} : 0 \right)_S. \end{aligned} \quad (2.2)$$

Here, as we noted in the footnote 1, we have to distinguish two different notations: italic f_{ν_α} for the case where we do not consider the neutrino and antineutrino flavor ratios independently, as they are *assumed* to be the same, and normal f_{ν_α} and $f_{\bar{\nu}_\alpha}$ for the case where we consider independently neutrino and antineutrino flavor ratios.

However, since the lifetime of the muon exceeds that of the charged pion by almost two orders of magnitude, it is also possible that the muon in the decay chain losses energy to the source environment by synchrotron radiation and interaction before it decays [39, 40]. If this happens, these low-energy muons will have a negligible contribution to the high energy neutrino flux. This will result in only ν_μ and $\bar{\nu}_\mu$ produced at the source, i.e.,

$$(f_{\nu_e}^S : f_{\nu_\mu}^S : f_{\nu_\tau}^S) \simeq (f_{\bar{\nu}_e}^S : f_{\bar{\nu}_\mu}^S : f_{\bar{\nu}_\tau}^S) \simeq \left(0 : \frac{1}{2} : 0\right)_S. \quad (2.3)$$

Again in this case we have the same flux for neutrinos and antineutrinos and we can again simply use the combined flavor ratio $(f_{\nu_e}^S : f_{\nu_\mu}^S : f_{\nu_\tau}^S) = (0 : 1 : 0)_S$.

2.2 $p\gamma$ production

On the other hand, if pions are produced mainly by $p\gamma$ interactions, the flux ratio of neutrinos and antineutrinos depends on the spectra of target photons, as discussed in [58]. If the target photons are very hard or thermal, multi-pion production would be more relevant and expected flavor ratio may become very similar to the pp case, as in eqs. (2.1) and (2.2). This is often expected in GRB and blazar models, see e.g. [59, 60].

However, if the target photons are sufficiently soft, the asymmetric process $p\gamma \rightarrow \Delta^+ \rightarrow n\pi^+$ will be the dominant source of neutrinos. Since π^- production is suppressed and π^+ decays do not produce $\bar{\nu}_e$, this lead to the flux flavor ratios at the source as

$$(f_{\nu_e}^S : f_{\nu_\mu}^S : f_{\nu_\tau}^S) \simeq \left(\frac{1}{3} : \frac{1}{3} : 0\right)_S, \quad (f_{\bar{\nu}_e}^S : f_{\bar{\nu}_\mu}^S : f_{\bar{\nu}_\tau}^S) \simeq \left(0 : \frac{1}{3} : 0\right)_S. \quad (2.4)$$

In this case neutrinos and antineutrinos exhibit quite different flavor ratios at the source, and their flavor ratios must be treated separately. Note that this is a simplified scenario since there would be always some contamination of the $\bar{\nu}_e$ flux in a realistic situation, see [36, 37]. However, we assume the ratios in eq. (2.4) for the $p\gamma$ source for the purpose of the illustration of the main point of this work.

Here again μ^+ 's decays can be damped by energy losses, in which case no antineutrinos would be produced at all at the source, leading to a even more asymmetric case. Therefore, as pointed out in [58], in general, to study $p\gamma$ sources, assumption of equal flavor ratios for neutrinos and antineutrinos is not appropriate.

2.3 Effect of oscillation

According to our current understanding, neutrino flavor eigenstates and mass eigenstates are connected by a mixing matrix U , so as they propagate mass eigenstates acquire relative phases that generate the so-called neutrino flavor oscillations. By propagating from the astrophysical source, where they are produced, to the Earth, where they are detected, these relative phases are washed out, so neutrinos arrive as an incoherent mixture of mass eigenstates [52]. We can thus write the flux flavor ratios at the Earth as

$$f_{\nu_\alpha}^\oplus(f_{\bar{\nu}_\alpha}^\oplus) = \sum_{\beta=e,\mu,\tau} \sum_{j=1,2,3} |U_{\alpha j}|^2 |U_{\beta j}|^2 f_{\nu_\beta}^S(f_{\bar{\nu}_\beta}^S) \quad (\alpha = e, \mu, \tau), \quad (2.5)$$

for neutrinos (antineutrinos).

So if we start at the source with equal fluxes for neutrinos and antineutrinos this equality will be preserved by the incoherent mixture that will arrive at the Earth. Conversely, if their original fluxes are unequal, one should not expect to have equal neutrino and antineutrino fluxes arriving on Earth. This feature has been studied in connection with the Glashow resonance as a way to probe production models [4, 61–67] and beyond the Standard Model physics [58]. In the next section we discuss how the difference in neutrino and antineutrino fluxes can affect the fitting of IceCube showers and track events in a way to mimic new physics. Since we do not know the production mechanism, it is imperative to fit the data without this limiting assumption, including extra parameters to allow for the possibility of a difference in neutrino and antineutrino fluxes for each flavor.

3 On the interpretation of IceCube data

We will show here that if the fluxes of high energy extraterrestrial neutrinos and antineutrinos that arrive at the Earth were unequal, by assuming their equality in the fit of IceCube data, one can obtain allowed regions in the flavor-ratio triangle at the Earth that lay outside the region expected by standard neutrino oscillations. This can be misinterpreted as a sign of new physics, while in fact it is simply due to an incorrect assumption about the fluxes. In practice, we are going to study four scenarios, which include two kinds of sources and two different exposures at IceCube.

In the first part of each analysis we simulate the number of showers and tracks that IceCube would observe given a particular source and exposure. In order to do this we fix the set of neutrino fractions at the source and then we derive the fractions at the Earth by using standard values for the neutrino mixing matrix. Afterwards, we use this as input to predict the number of track and shower events for a given energy bin of the IceCube detector. In fact, we just use the fractions to scale up a set of normalized values of showers and tracks that we have already computed following the detailed prescriptions of ref. [15] (see appendix B for details). In these computations we have assumed that neutrinos and antineutrinos of any flavor α follow the same energy spectrum, so that we can parameterize the sum of the fluxes as

$$\frac{d\Phi(E, \gamma, C_r)}{dE} = \frac{C_r}{10^8} \left(\frac{E}{100 \text{ TeV}} \right)^{2-\gamma} \frac{1}{E^2} [\text{GeV}^{-1} \text{ cm}^{-2} \text{ str}^{-1} \text{ s}^{-1}], \quad (3.1)$$

where E is the neutrino energy, C_r is a normalization constant and γ is the spectral index. Thus, the neutrino (antineutrino) flavor fluxes at the Earth are

$$\frac{d\Phi_{\nu_\alpha(\bar{\nu}_\alpha)}^\oplus(E, \gamma, C_r)}{dE} = f_{\nu_\alpha(\bar{\nu}_\alpha)}^\oplus \frac{d\Phi(E, \gamma, C_r)}{dE}, \quad (3.2)$$

where $f_{\nu_\alpha(\bar{\nu}_\alpha)}^\oplus$ are the normalized neutrino fractions at the Earth. For each simulation of the expected data we fix the spectral index to $\gamma = 2.5$ and the total number of events of astrophysical neutrinos to $N_a = 18 \times 10$ (100) in the energy interval [28 TeV, 10 PeV]. These numbers are motivated by the best fit point of IceCube given by the combined maximum-likelihood analysis of ref. [18], which corresponds to 18 astrophysical neutrinos in 988 days in the energy range [28 TeV, 10 PeV], so we use 10 (100) times more exposure to try to simulate future observations.

Furthermore, we also consider the background from atmospheric neutrinos and atmospheric muons. Again, we mostly follow ref. [15] (see appendix C for details). Thus, in

each analysis we fix the number of atmospheric neutrinos to $N_\nu = 6.6$ and the number of atmospheric muons to $N_\mu = 8.4$ per 18 astrophysical neutrino events.² This was done in order to match the central values obtained by IceCube in the interval [28 TeV, 10 PeV] after 988 days of data taking [3]. The uncertainty associated to these numbers are not considered in this analysis but we have checked that this effect, that may be added through nuisance parameters in the fit, does not change our final conclusions.

Besides, it would be necessary to take into account the potential effects associated to the experimental misidentification of tracks as showers, as done in ref. [15] where the rates of 20 and 30% were considered based on [57]. In this work, we set the track to shower miss-identification rate to be somewhat more optimistic value, 10%, which is applied to every contribution. We believe that moderate modifications of this rate do not affect essentially our final conclusions. The final number of showers and tracks computed in this way will simulate the observed data measured by IceCube. Finally, let us emphasize that we consider only one realization of the simulation for each scenario (see appendix A for more details).

In the second part of each analysis we study the fit of the simulated data. Thus, we use the same approach described above to compute the number of showers and tracks, but now considering floating values of the normalization parameter N_a , the spectral index γ and the neutrino fractions at the Earth $f_{\nu_\alpha(\bar{\nu}_\alpha)}^\oplus$. For each scanned point in this parameter space we evaluate a binned likelihood function, that we extreme in order to find the best fit point and the corresponding confidence level regions of the relevant parameters. In the fit procedure we make the key assumption that the neutrino and antineutrino fluxes are equal for all flavors, i.e., $f_{\nu_\alpha}^\oplus = f_{\bar{\nu}_\alpha}^\oplus = f_{\nu_\alpha}^\oplus/2$. Details about the fit procedure can be found in appendix A.

3.1 A possible scenario fitted with the wrong assumption

We start by discussing a theoretically viable example. Let's assume here that the neutrino fluxes are produced at the source by the mechanism $p\gamma$ of photo-disintegration. This corresponds to fixing the neutrino and antineutrino flavor fractions at the source as

$$(f_{\nu_e}^S : f_{\nu_\mu}^S : f_{\nu_\tau}^S) = \left(\frac{1}{3} : \frac{1}{3} : 0\right)_S, \quad (f_{\bar{\nu}_e}^S : f_{\bar{\nu}_\mu}^S : f_{\bar{\nu}_\tau}^S) = \left(0 : \frac{1}{3} : 0\right)_S. \quad (3.3)$$

For definiteness, we also fix the oscillation parameters to

$$\sin^2 \theta_{12} = 0.31, \quad \sin^2 \theta_{23} = 0.60, \quad \sin^2 \theta_{13} = 0.02, \quad \delta = 3\pi/2,$$

in order to obtain the theoretical predicted propagated flavor fractions at the Earth,

$$(f_{\nu_e}^{\oplus T} : f_{\nu_\mu}^{\oplus T} : f_{\nu_\tau}^{\oplus T}) = (0.25 : 0.21 : 0.21)_\oplus, \quad (f_{\bar{\nu}_e}^{\oplus T} : f_{\bar{\nu}_\mu}^{\oplus T} : f_{\bar{\nu}_\tau}^{\oplus T}) = (0.06 : 0.15 : 0.12)_\oplus, \quad (3.4)$$

where the superscript T here means theoretically expected value. Note that, as expected, the sum of the neutrino (antineutrino) fractions at the Earth coincide with the sum of the neutrino (antineutrino) fractions at the source, and similarly for antineutrinos. Also $f_{\nu_\alpha}^{\oplus T} + f_{\bar{\nu}_\alpha}^{\oplus T} \approx 1/3$, albeit $f_{\nu_\alpha}^{\oplus T} \neq f_{\bar{\nu}_\alpha}^{\oplus T}$. As we said before, these fractions fix the *mock-data* for the fit. Our binned maximum-likelihood fit (see appendix A) of this data involves four free parameters: the global normalization, N_a^F , the spectral index, γ^F , and the $\nu_e + \bar{\nu}_e$ and $\nu_\mu + \bar{\nu}_\mu$ flavor fractions at the Earth $f_{\nu_e}^{\oplus F}$, $f_{\nu_\mu}^{\oplus F}$ with the constraint $f_{\nu_\tau}^{\oplus F} = 1 - f_{\nu_e}^{\oplus F} - f_{\nu_\mu}^{\oplus F}$. The superscript F here means fit

²Indeed, we fix these numbers to $N_\nu = 6.6 \times 10(100)$ and $N_\mu = 8.4 \times 10(100)$ in order to correct for the two exposures that we are simulating.

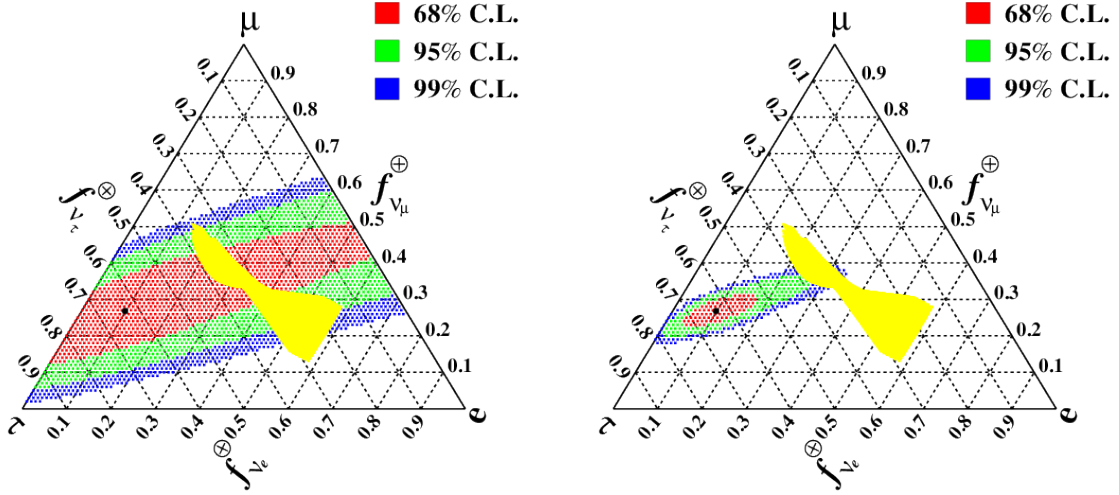


Figure 2. Regions allowed at 68% (red), 95% (green) and 99% C.L. (blue) in the parameter space of the astrophysical flavor ratios $(f_{\nu_e}^{\oplus}, f_{\nu_\mu}^{\oplus}, f_{\nu_\tau}^{\oplus})$ at the Earth. On the left (right) panel we used a total number of 180 (1800) astrophysical neutrino events. The input data was simulated for the $p\gamma$ production scenario with $(f_{\nu_e}^S : f_{\nu_\mu}^S : f_{\nu_\tau}^S) = (\frac{1}{3} : \frac{1}{3} : 0)_S$, $(f_{\bar{\nu}_e}^S : f_{\bar{\nu}_\mu}^S : f_{\bar{\nu}_\tau}^S) = (0 : \frac{1}{3} : 0)_S$ and $\sin^2 \theta_{12} = 0.31$, $\sin^2 \theta_{23} = 0.60$, $\sin^2 \theta_{13} = 0.02$, $\delta = 3\pi/2$ and the data was fitted with the wrong assumption that all neutrino and antineutrino flavor fluxes are the same at the Earth. We also show the region allowed by the standard oscillation hypothesis (same as figure 1).

value. As the result of the fit we get the best fit point: $N_a^F = 17.91 \times 10(100)$, $\gamma^F = 2.48$, $f_{\nu_e}^{\oplus F} = 0.098$ and $f_{\nu_\mu}^{\oplus F} = 0.27$.

We show the results of our fit in figure 2 for the cases where the total number of astrophysical neutrino events are assumed to be 180 (left panel) and 1800 (right panel). It is interesting to notice that, with the wrong assumption about neutrino and antineutrino fluxes, to fit the *mock-data* corresponding to the $p\gamma$ scenario requires that the best fit point for the flux flavor fractions falls outside of the standard central region of the flavor-ratio triangle, as can be clearly seen by the solid black circles in figure 2. In this figure we show the allowed regions at 68% (red), 95% (green) and 99% C.L. (blue) in the flavor-ratio triangle spanned in the $(f_{\nu_e}^{\oplus}, f_{\nu_\mu}^{\oplus}, f_{\nu_\tau}^{\oplus})$ parameter space. The limited region predicted by standard oscillations, as shown before in figure 1, is also depicted in yellow. In the left panel, we note that despite that the wrong assumption (of equal fluxes of neutrino and antineutrinos) was made, the result of the fit is quite good such that this assumption can not be statistically rejected even at 1σ confidence level. However, in the right panel, when ten times more statistics is used, just one small part of the yellow zone is compatible with the boundary of the 2σ confidence level region.

How can we understand this result? Let's see how it arises from the fact that the simulated data, producing flavor fractions at the Earth $f_{\nu_\alpha}^{\oplus T} \neq f_{\bar{\nu}_\alpha}^{\oplus T}$, is fitted using $f_{\nu_\alpha}^{\oplus F} = f_{\bar{\nu}_\alpha}^{\oplus F} = f_{\nu_\alpha}^{\oplus F}/2$ at the Earth. The argument goes as follow. The spectrum of shower events from $\bar{\nu}_e$, thanks to the Glashow Resonance, is quite different from the spectra of shower events from ν_e , ν_τ and $\bar{\nu}_\tau$ (see figure 6). With enough statistics, as it is the case of our simulated events, we expect the fitted fractions to reproduce theory fractions. Although the Glashow Resonance is localized around one or two energy bins we note that its effect is going to affect the fit of the whole energy range because it determines the overall normalization

of $\bar{\nu}_e$ flux. Later we can check this hypothesis from the comparison between the fit and the expected fractions. So the $\bar{\nu}_e$ shower event distribution will impose

$$\frac{f_{\nu_e}^{\oplus F}}{2} \approx f_{\bar{\nu}_e}^{\oplus T} \simeq 0.06, \quad (3.5)$$

while since ν_e , ν_τ and $\bar{\nu}_\tau$ shower events have similar energy dependence (see figure 6) they impose

$$\frac{f_{\nu_e}^{\oplus F}}{2} + f_{\nu_\tau}^{\oplus F} \approx f_{\nu_e}^{\oplus T} + f_{\nu_\tau}^{\oplus T} + f_{\bar{\nu}_\tau}^{\oplus T}, \quad (3.6)$$

and track events will fix

$$f_{\nu_\mu}^{\oplus F} \approx f_{\nu_\mu}^{\oplus T} + f_{\bar{\nu}_\mu}^{\oplus T} \simeq 0.36. \quad (3.7)$$

By combining equations (3.5) and (3.6), and $f_{\nu_e}^{\oplus T} \simeq 0.25$ from eq. (3.4), we get

$$\begin{aligned} f_{\nu_\tau}^{\oplus F} &\approx f_{\nu_\tau}^{\oplus T} + f_{\bar{\nu}_\tau}^{\oplus T} + f_{\nu_e}^{\oplus T} - f_{\bar{\nu}_e}^{\oplus T}, \\ &\approx \frac{1}{3} + f_{\nu_e}^{\oplus T} - f_{\bar{\nu}_e}^{\oplus T} \simeq 0.52, \end{aligned} \quad (3.8)$$

where we have used that $f_{\nu_\tau}^{\oplus T} + f_{\bar{\nu}_\tau}^{\oplus T} \sim 1/3$. We see that the output of the fit is consistent with the rough estimation given by eqs. (3.5)–(3.7) based on our event distribution considerations for showers of different flavors and the importance of the Glashow Resonance for the fit. Notice that the previous equations do not include the relative weight of the distributions, we have checked that by considering this extra information the agreement is even better.

The conclusions derived from this case will certainly hold for a variety of other examples. For instance, if no antineutrinos at all were produced at the source, and consequently none would arrive at the Earth (the case of μ^+ damping), we would expect to fit $f_{\nu_e}^{\oplus F} \approx f_{\bar{\nu}_e}^{\oplus T} \sim 0$, leading to a best fit point again well outside the standard region of the flavor-ratio triangle.

3.2 Re-thinking current results

In ref. [18] IceCube finds, assuming $f_{\nu_\alpha}^{\oplus} = f_{\bar{\nu}_\alpha}^{\oplus} = f_{\nu_\alpha}^{\oplus}/2$, the best fit point for the neutrino flavor ratios at the Earth to be $(f_{\nu_e}^{\oplus} : f_{\nu_\mu}^{\oplus} : f_{\nu_\tau}^{\oplus}) \simeq (0.5 : 0.5 : 0.0)$. While it is not yet statistically significant, this point is outside the *standard region* of figure 1. Let's assume, for the sake of discussion, that these numbers will be confirmed with higher significance by future data. Is this a sign of exotic physics (due to some non-standard properties of neutrinos) or can this be explain by standard physics? Can we find neutrino and antineutrino flavor ratios at the source that can give this result at the Earth if fitted with the wrong assumption?

Indeed, we can explain the IceCube best fit of neutrino fractions by considering only standard neutrino physics plus an asymmetric source of neutrinos. Take, for instance, the following flavor fractions at the source

$$(f_{\nu_e}^S : f_{\nu_\mu}^S : f_{\nu_\tau}^S) = (0 : 0.3 : 0)_S, \quad (f_{\bar{\nu}_e}^S : f_{\bar{\nu}_\mu}^S : f_{\bar{\nu}_\tau}^S) = (0.4 : 0.3 : 0)_S. \quad (3.9)$$

We note that if we do not distinguish neutrinos and antineutrinos, the flavor ratios given in (3.9) correspond to $(f_{\nu_e}^S : f_{\nu_\mu}^S : f_{\nu_\tau}^S) = (0.4 : 0.3 : 0.3)$ which gives $(f_{\nu_e}^{\oplus} : f_{\nu_\mu}^{\oplus} : f_{\nu_\tau}^{\oplus}) \simeq (0.34 : 0.34 : 0.32)$, very close to the central point of the triangle. Below we will see that this point could be mistakenly excluded due to the wrong assumption provided that we will have enough statistics, giving (fake) best fit outside the standard allowed region.

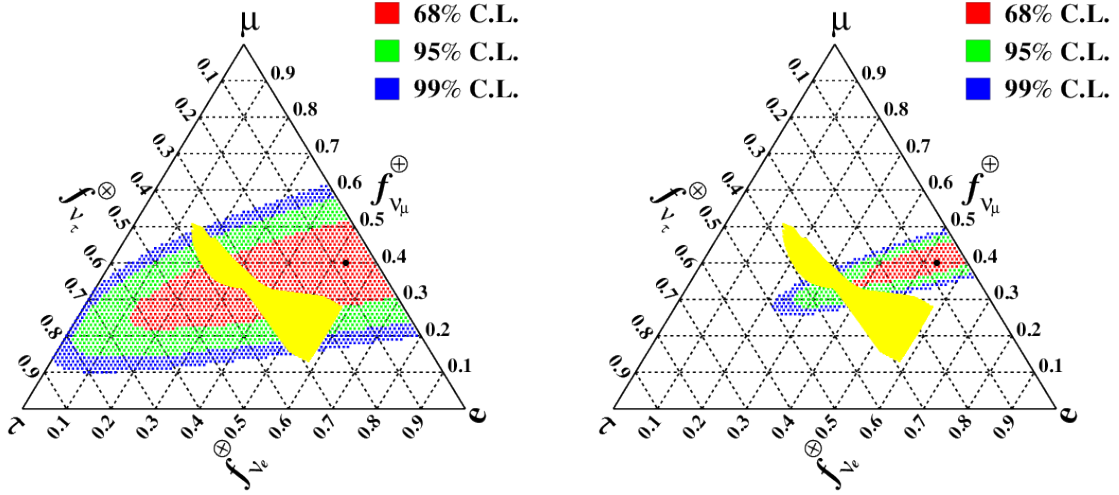


Figure 3. Allowed regions at 68% (red), 95% (green) and 99% C.L. (blue) for the astrophysical flavor ratios $(f_{\nu_e}^\oplus, f_{\nu_\mu}^\oplus, f_{\nu_\tau}^\oplus)$ at the Earth. On the left (right) panel we used a total number of 180 (1800) astrophysical neutrino events. The input data was simulated for a fictitious production scenario with $(f_{\nu_e}^S : f_{\nu_\mu}^S : f_{\nu_\tau}^S) = (0 : 0.3 : 0)_S$, $(f_{\bar{\nu}_e}^S : f_{\bar{\nu}_\mu}^S : f_{\bar{\nu}_\tau}^S) = (0.3 : 0.4 : 0)_S$, and $\sin^2 \theta_{12} = 0.31$, $\sin^2 \theta_{23} = 0.60$, $\sin^2 \theta_{13} = 0.02$, $\delta = 3\pi/2$. The data was fitted with the wrong assumption that all neutrino and antineutrino flavor fluxes are the same at the Earth. We also show the region predicted by the standard oscillation hypothesis (same as in figure 1).

Note that this scenario is in principle possible if we consider the case where neutrinos are coming from the two kinds of sources, namely the combination of the pion decay with muon dump in pp scenario and neutron decay source with the ratios of the former to the latter equal to 4 : 3. In such a case, the pp source leads to equal fluxes of ν_μ and $\bar{\nu}_\mu$ whereas the neutron source leads to pure $\bar{\nu}_e$ flux. Now, fix the same oscillation parameters as before to propagate this to the Earth. The result at the Earth will be

$$(f_{\nu_e}^{\oplus T} : f_{\nu_\mu}^{\oplus T} : f_{\nu_\tau}^{\oplus T}) = (0.06 : 0.13 : 0.11)_\oplus, \quad (f_{\bar{\nu}_e}^{\oplus T} : f_{\bar{\nu}_\mu}^{\oplus T} : f_{\bar{\nu}_\tau}^{\oplus T}) = (0.28 : 0.21 : 0.21)_\oplus. \quad (3.10)$$

We have generated *mock data* in accordance with this theoretical prediction at the Earth assuming $N_a^T = 18 \times 10(100)$ astrophysical neutrinos and $\gamma^T = 2.5$. Finally, we have fit the expected number of events using the standard approach of IceCube, i.e., assuming the neutrino and antineutrino fractions to be equal at the Earth.

We show our results in figure 3. The result of our fit, with this wrong assumption, is $(f_{\nu_e}^{\oplus F} : f_{\nu_\mu}^{\oplus F} : f_{\nu_\tau}^{\oplus F}) = (0.52 : 0.41 : 0.07)$, $N_a^F = 179$ and $\gamma^F = 2.46$. These results are in close agreement with the IceCube fit, as shown in figure 3. Furthermore, this is consistent with eqs. (3.5)–(3.7). We conclude that there could be a standard physics explanation for this point as long as we relax the constraint that imposes flavor fraction to be the same for neutrinos and antineutrinos. We have checked explicitly that if we perform a fit by varying independently neutrino and antineutrino fluxes, we recover the input fractions and the allowed regions sit around the central part of the flavor-ratio triangle.

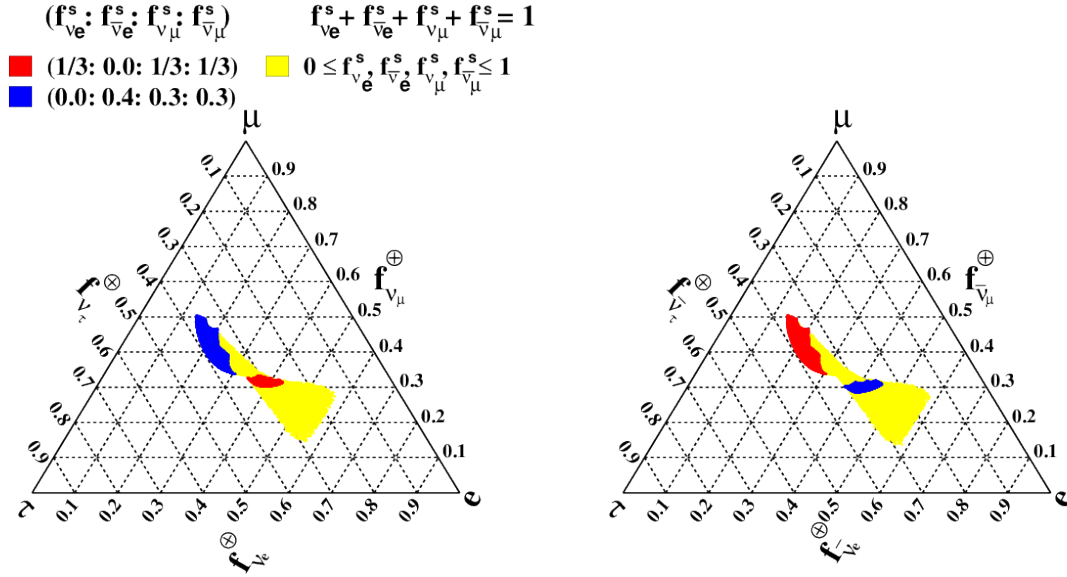


Figure 4. On the right (left) panel we present the currently allowed regions for the flux flavor ratios $f_{\nu_e}^{\oplus}, f_{\nu_\mu}^{\oplus}, f_{\nu_\tau}^{\oplus}$ ($f_{\bar{\nu}_e}^{\oplus}, f_{\bar{\nu}_\mu}^{\oplus}, f_{\bar{\nu}_\tau}^{\oplus}$) at the Earth by various high energy neutrino production mechanisms. We let neutrino mixing parameters vary with the current 3σ allowed regions [45]. We have normalized the total neutrino (left panel) and antineutrino (right panel) flavor fractions at the Earth to 1 separately for each point in order to show them in this manner. The red regions correspond to the case where $(f_{\nu_e}^S, f_{\nu_\mu}^S, f_{\nu_\tau}^S) = (1/3 : 1/3 : 0)$ and $(f_{\bar{\nu}_e}^S, f_{\bar{\nu}_\mu}^S, f_{\bar{\nu}_\tau}^S) = (0 : 1/3 : 0)$ and the blue one corresponds to $(f_{\nu_e}^S, f_{\nu_\mu}^S, f_{\nu_\tau}^S) = (0 : 0.3 : 0)$ and $(f_{\bar{\nu}_e}^S, f_{\bar{\nu}_\mu}^S, f_{\bar{\nu}_\tau}^S) = (0.4 : 0.3 : 0)$.

4 Discussions and conclusions

Whether pp or $p\gamma$ interactions (or some combination) in Fermi engines are the sources of these neutrinos will be probably established by data, as soon as enough statistics is accumulated by IceCube or its successors IceCube-Gen2 [68] or KM3NeT2.0 [69]. Many authors [4, 58, 61–67] have stressed the importance of the Glashow resonance as a discriminator.

In this paper we show that one must be careful when discussing IceCube flavor ratio results, that at the moment assume neutrino and antineutrino flavor ratios at the Earth are equal, as a way to probe new physics in the neutrino sector. The flavor ratios for neutrinos and antineutrinos can be quite different as we do not know how they are produced in the astrophysical environment, so the flavor ratios for neutrinos and antineutrinos at the Earth also can be quite distinct, as can be seen in figure 4 where the expected normalized ratios for neutrinos (left panel) and antineutrinos (right panel) are shown separately for the two representative cases we considered in this work, $(f_{\nu_e}^S : f_{\nu_\mu}^S : f_{\nu_\tau}^S) = (1/3 : 1/3 : 0)_S$ in red and $(0 : 0.4 : 0.3 : 0.3)_S$ in blue. Since in figure 4 we only show normalized ratios, the information about the total fraction of neutrinos (antineutrinos) for each point is not present. A possible way of showing the neutrino and antineutrino ratios without losing information is by using 15 triangle plots with axes given by triplets $(f_{\nu_i}, f_{\nu_j}, 1 - f_{\nu_i} - f_{\nu_j})$ where ν_i runs over neutrino and antineutrino flavors.³

³Indeed, we may consider that effectively we have only four interesting ratios $f_{\nu_e}, f_{\bar{\nu}_e}, f_{\nu_\mu}$ and f_{ν_τ} , which reduces the number of triangle plots to 6. This because the spectra of muon and tau neutrinos are quite similar to their anti-neutrino counterpart.

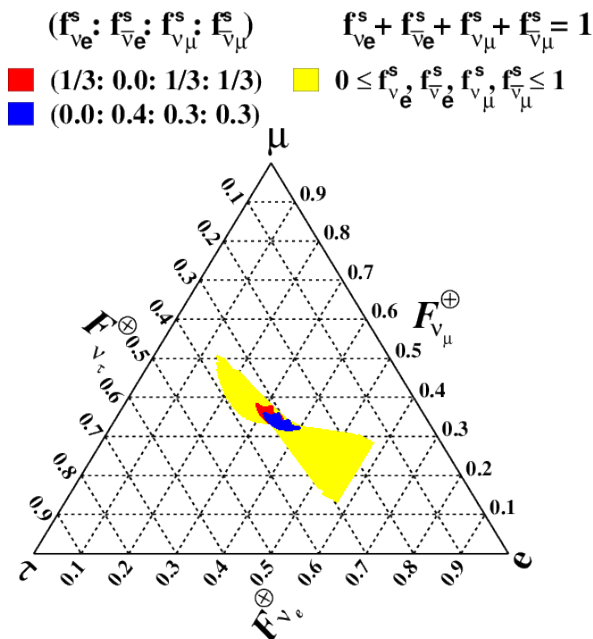


Figure 5. Same as figure 4 but for the sum of the neutrino and antineutrino fractions, $\mathbf{F}_{\nu_\alpha}^\oplus = \mathbf{f}_{\nu_\alpha}^\oplus + \mathbf{f}_{\bar{\nu}_\alpha}^\oplus$.

In particular, we see that the standard case for $p\gamma$ production (in red) or the example we provided that could be consistent with the current best fit point of IceCube (in blue), generate neutrino and antineutrino (normalized) ratios that cover different zones in the respective flavor-ratio triangles.

On the other hand, the sum of the neutrino and antineutrino flavor ratios at the Earth spread over a small region around the center of the triangle, see figure 5. However, when we fit the data generated by these scenarios assuming equality between neutrino and antineutrino ratios at the Earth, we obtain that the best fit point lies outside the central region of the respective triangle plot, as we showed in figures 2 and 3. Thus, this wrong assumption could lead to the conclusion that new physics is necessary in the neutrino sector, which is not necessarily the case.

Although at the current exposure of IceCube the assumption that neutrino and antineutrino flavor fractions are the same at the Earth when fitting the data seems quite reasonable, because most of the triangle is still allowed by the current data (including the standard region), this will have to change in the future when more data will be available. In particular, in order to be able to disentangle different production mechanisms at the source from new physics in the neutrino sector, it is imperative to work with the measured neutrino and antineutrino flavor ratios at the Earth, separately.

Acknowledgments

We thank Olga Mena and Sergio Palomares-Ruiz for useful discussions on the computation of number of events induced by high energy astrophysical neutrinos. We also acknowledge Kohta Murase and Walter Winter for useful comments. This work was supported by Fundação de Amparo à Pesquisa do Estado de São Paulo (FAPESP), Fundação Carlos Chagas Filho de

Amparo à Pesquisa do Estado do Rio de Janeiro (FAPERJ) and Conselho Nacional de Ciência e Tecnologia (CNPq). H.N. and R.Z.F. thank the Kavli Institute for Theoretical Physics in UC Santa Barbara for its hospitality, where part of this work was initiated. This research was supported in part by the National Science Foundation under Grant No. NSF PHY11-25915, and European Union’s Horizon 2020 research and innovation programme under Marie Skłodowska-Curie grant agreement No. 674896.

A Binned likelihood

In order to compute both the best fit point plus the confidence level regions for the relevant free parameters, we consider as test statistics the function [70],

$$-2 \ln \lambda(\theta) = 2 \sum_{k=\text{sh, tr}} \sum_{i=1}^{N_{\text{bins}}} \left[\mu_{k,i}(\theta) - n_{k,i} + n_{k,i} \ln \frac{n_{k,i}}{\mu_{k,i}(\theta)} \right], \quad (\text{A.1})$$

where $N_{\text{bins}} = 14$ is the number of logarithmically uniform bins in the range [28 TeV, 10 PeV]. The numbers $n_{k,i}$ correspond to the *observed* events of topology k , shower or track, in the i -th bin. Thus, these numbers just depend on the assumption about the particular scenario considered for each analysis. On the other hand, the values $\mu_{k,i}(\theta)$ are the floating number of events of topology k in the i -th bin. Accordingly, these numbers depend on the free parameters of the fit, which in general are given by $\theta = (N_a, \gamma, f_{\nu_\alpha(\bar{\nu}_\alpha)})$.

Thus, the best fit point is obtained by minimizing eq. (A.1) with respect to the free parameters of the fit. Later, the confidence regions are computed by considering proper threshold values of the function $2\Delta \ln \lambda(\theta) = -2 \ln \lambda(\theta) + 2 \ln \lambda(\theta_{\text{best-fit}})$, which are tabulated in [70] and depend on the number of free parameters. For instance, for the triangle plots we use $2\Delta \ln \lambda(\theta) = 2.30, 5.99$ and 6.63 for the C.L. regions at $1\sigma, 2\sigma$ and 3σ correspondingly.

Notice that during the analysis of the four scenarios considered in section 3, which account for two different sources times two different exposures, we consider only one simulation of the *observed* data in each case. The number of events at each bin is given by the theoretical expected values obtained directly from the computation of flux times cross section times detector effects.

Clearly, this procedure may be improved. For instance, we could consider multiple realizations of the data simulation by using poisson distributed numbers with mean values given by the theoretical predictions. Then, we could use the density maps containing the best fit point of each realization in order to find the global best fit and the confidence level regions. Also, we may consider the uncertainty on the numbers associated to the background predictions by including nuisance parameters into the definition of the likelihood. Indeed, we have checked both options and we have found that the general results of our analysis are not modified. The most clear effects are that the confidence level regions are not necessarily well shaped ellipses and cover slightly bigger areas, however they still keep the same basic features that we found with our simpler analysis. We believe that our simplified approach to show only the case of the single realization is sufficient to illustrate the main point of this work.

B Astrophysical neutrinos

We assume that the flux of astrophysical neutrinos at Earth is given by eq. (3.1). In order to generate standard tables of shower and track events, we normalize the value of C_r

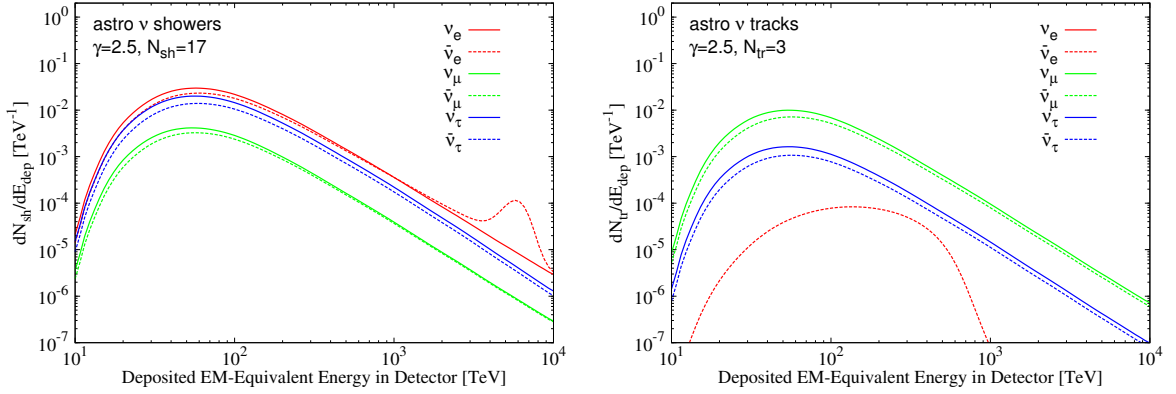


Figure 6. Contribution of each flavor to shower (left panel) and track (right panel) events induced by astrophysical neutrinos as a function of the deposited energy in the IceCube detector, as simulated by us.

such that 20 astrophysical neutrinos are obtained in the interval [10 TeV, 10 PeV] and we consider that the six independent neutrino fractions at Earth are equal to 1/6. In figure 6 we show the contributions of each flavor to the spectrum of showers and tracks for $\gamma = 2.5$ and $N_a = 20$, where N_a is the total number of events with astrophysical origin. Notice that the electron-neutrino does not contribute to the tracks because there is no interaction channel that produces a muon or a tau. All the rest can produce both showers and tracks. These results are obtained from the convolution of each neutrino flux with the corresponding neutrino-nucleon cross sections plus detector effects, for which we have followed tightly the reference [15] and references therein.

C High-energy neutrino background

With respect to the background, we consider the contribution of electron and muon atmospheric neutrinos plus the fake contribution from atmospheric muons. In the corresponding tables we have split the contribution of neutrinos and anti-neutrinos. To compute the electron and muon neutrino atmospheric flux we consider the expressions given in [71],

$$\frac{d\Phi_\alpha(E_\nu)}{dE} = C_\alpha \left(\frac{E_\nu}{1 \text{ GeV}} \right)^{-(g_0 + g_1 y + g_2 y^2)} \quad \text{with} \quad y = \frac{E_\nu}{1 \text{ GeV}}, \quad (\text{C.1})$$

where the values of C_α , g_0 , g_1 and g_2 can be found in this reference, for each flavor. We consider equal contributions from neutrinos and anti-neutrinos. In order to include the experimental veto for downgoing atmospheric muon-neutrinos we follow the algorithm showed in section III of [15], which is based on the following references [72, 73].

Similarly, for the muon flux we also follow [15], so we consider the absolute number of tracks produced from the atmospheric muon background as given by

$$\frac{dN(E_\nu)}{dE} = \begin{cases} C_\mu (E_\nu/1 \text{ GeV})^{-\gamma_\mu} & \text{for } E > E_{\min} \\ C_\mu (E_{\min}/1 \text{ GeV})^{-\gamma_\mu - 18.5} (E_\nu/1 \text{ GeV})^{18.5} & \text{for } E < E_{\min} \end{cases} \quad (\text{C.2})$$

where

$$\gamma_\mu = \frac{\log(21)}{(\log(60 \text{ TeV}/E_{\min}))} + 1 \quad \text{and} \quad E_{\min} = 28 \text{ TeV}.$$

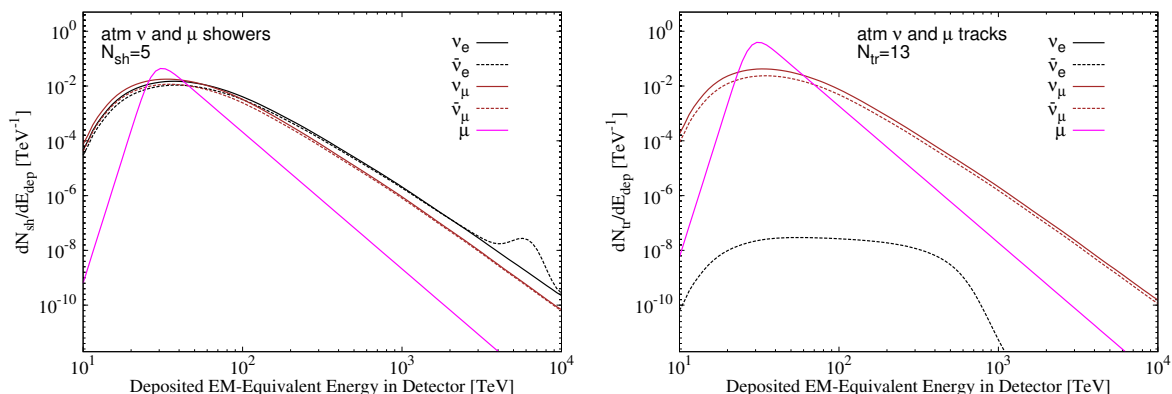


Figure 7. Background contribution to showers (left panel) and tracks (right panel). Notice that the y-axis has been extended to $10^{-14} \text{ GeV}^{-1}$ in order to cover interesting features of the background.

For each analysis showed in the body of the paper we fix the number of atmospheric neutrinos to $N_\nu = 6.6$ and the number of atmospheric muons to $N_\mu = 8.4$ in order to match the central values obtained by IceCube in the interval $[28 \text{ TeV}, 10 \text{ PeV}]$ after 988 days of data taking [3]. Notice that in the later reference these central values are reported with their respective uncertainties, however we do not consider this information in the paper. Nonetheless, we have checked that the effect of these uncertainties, included as nuisance parameters into the fit, do not affect our final conclusions.

We show the background contributions to shower and tracks in figure 7. The neutrino curves are obtained by performing the convolution of the fluxes given in eq. (C.1) with the neutrino-nucleon cross sections in the same way as we do for astrophysical neutrinos. Then, it is natural to observe some similarities between the neutrino spectra of figures 6 and 7. The muon spectrum on the other hand is obtained directly from eq. (C.2) and turns out to be quite distinct.

References

- [1] ICECUBE collaboration, M.G. Aartsen et al., *First observation of PeV-energy neutrinos with IceCube*, *Phys. Rev. Lett.* **111** (2013) 021103 [[arXiv:1304.5356](#)] [[INSPIRE](#)].
- [2] ICECUBE collaboration, M.G. Aartsen et al., *Evidence for high-energy extraterrestrial neutrinos at the IceCube detector*, *Science* **342** (2013) 1242856 [[arXiv:1311.5238](#)] [[INSPIRE](#)].
- [3] ICECUBE collaboration, M.G. Aartsen et al., *Observation of high-energy astrophysical neutrinos in three years of IceCube data*, *Phys. Rev. Lett.* **113** (2014) 101101 [[arXiv:1405.5303](#)] [[INSPIRE](#)].
- [4] A. Bhattacharya, R. Gandhi, W. Rodejohann and A. Watanabe, *The Glashow resonance at IceCube: signatures, event rates and pp vs. $p\gamma$ interactions*, *JCAP* **10** (2011) 017 [[arXiv:1108.3163](#)] [[INSPIRE](#)].
- [5] A. Esmaili and P.D. Serpico, *Are IceCube neutrinos unveiling PeV-scale decaying dark matter?*, *JCAP* **11** (2013) 054 [[arXiv:1308.1105](#)] [[INSPIRE](#)].
- [6] C.S. Fong, H. Minakata, B. Panes and R. Zukanovich Funchal, *Possible interpretations of IceCube high-energy neutrino events*, *JHEP* **02** (2015) 189 [[arXiv:1411.5318](#)] [[INSPIRE](#)].
- [7] E. Roulet, G. Sigl, A. van Vliet and S. Mollerach, *PeV neutrinos from the propagation of ultra-high energy cosmic rays*, *JCAP* **01** (2013) 028 [[arXiv:1209.4033](#)] [[INSPIRE](#)].

- [8] I. Cholis and D. Hooper, *On the origin of IceCube's PeV neutrinos*, *JCAP* **06** (2013) 030 [[arXiv:1211.1974](#)] [[INSPIRE](#)].
- [9] O.E. Kalashev, A. Kusenko and W. Essey, *PeV neutrinos from intergalactic interactions of cosmic rays emitted by active galactic nuclei*, *Phys. Rev. Lett.* **111** (2013) 041103 [[arXiv:1303.0300](#)] [[INSPIRE](#)].
- [10] F.W. Stecker, *PeV neutrinos observed by IceCube from cores of active galactic nuclei*, *Phys. Rev. D* **88** (2013) 047301 [[arXiv:1305.7404](#)] [[INSPIRE](#)].
- [11] K. Murase, M. Ahlers and B.C. Lacki, *Testing the hadronuclear origin of PeV neutrinos observed with IceCube*, *Phys. Rev. D* **88** (2013) 121301 [[arXiv:1306.3417](#)] [[INSPIRE](#)].
- [12] O. Mena, S. Palomares-Ruiz and A.C. Vincent, *Flavor composition of the high-energy neutrino events in IceCube*, *Phys. Rev. Lett.* **113** (2014) 091103 [[arXiv:1404.0017](#)] [[INSPIRE](#)].
- [13] M. Bustamante, J.F. Beacom and W. Winter, *Theoretically palatable flavor combinations of astrophysical neutrinos*, *Phys. Rev. Lett.* **115** (2015) 161302 [[arXiv:1506.02645](#)] [[INSPIRE](#)].
- [14] A. Palladino, G. Pagliaroli, F.L. Villante and F. Vissani, *What is the flavor of the cosmic neutrinos seen by IceCube?*, *Phys. Rev. Lett.* **114** (2015) 171101 [[arXiv:1502.02923](#)] [[INSPIRE](#)].
- [15] S. Palomares-Ruiz, A.C. Vincent and O. Mena, *Spectral analysis of the high-energy IceCube neutrinos*, *Phys. Rev. D* **91** (2015) 103008 [[arXiv:1502.02649](#)] [[INSPIRE](#)].
- [16] A. Watanabe, *The spectrum and flavor composition of the astrophysical neutrinos in IceCube*, *JCAP* **08** (2015) 030 [[arXiv:1412.8264](#)] [[INSPIRE](#)].
- [17] N. Kawanaka and K. Ioka, *Neutrino flavor ratios modified by cosmic ray secondary acceleration*, *Phys. Rev. D* **92** (2015) 085047 [[arXiv:1504.03417](#)] [[INSPIRE](#)].
- [18] ICECUBE collaboration, M.G. Aartsen et al., *A combined maximum-likelihood analysis of the high-energy astrophysical neutrino flux measured with IceCube*, *Astrophys. J.* **809** (2015) 98 [[arXiv:1507.03991](#)] [[INSPIRE](#)].
- [19] C.-Y. Chen, P.S. Bhupal Dev and A. Soni, *Two-component flux explanation for the high energy neutrino events at IceCube*, *Phys. Rev. D* **92** (2015) 073001 [[arXiv:1411.5658](#)] [[INSPIRE](#)].
- [20] E. Waxman and J.N. Bahcall, *High-energy neutrinos from cosmological gamma-ray burst fireballs*, *Phys. Rev. Lett.* **78** (1997) 2292 [[astro-ph/9701231](#)] [[INSPIRE](#)].
- [21] E. Waxman and J.N. Bahcall, *High-energy neutrinos from astrophysical sources: an upper bound*, *Phys. Rev. D* **59** (1999) 023002 [[hep-ph/9807282](#)] [[INSPIRE](#)].
- [22] L. Bento, P. Keranen and J. Maalampi, *Neutrino mixing scenarios and AGN*, *Phys. Lett. B* **476** (2000) 205 [[hep-ph/9912240](#)] [[INSPIRE](#)].
- [23] K. Bechtol, M. Ahlers, M. Di Mauro, M. Ajello and J. Vandenbroucke, *Evidence against star-forming galaxies as the dominant source of IceCube neutrinos*, [arXiv:1511.00688](#) [[INSPIRE](#)].
- [24] D. Grasso, D. Gaggero, A. Marinelli, A. Urbano and M. Valli, *Gamma-ray and neutrino diffuse emissions of the galaxy above the TeV*, *PoS(ICRC2015)489* [[arXiv:1507.07796](#)] [[INSPIRE](#)].
- [25] M. Kadler et al., *Coincidence of a high-fluence blazar outburst with a PeV-energy neutrino event*, *Nature Phys.* **12** (2016) 807 [[arXiv:1602.02012](#)] [[INSPIRE](#)].
- [26] R. Moharana, S. Razzaque, N. Gupta and P. Meszaros, *High-energy neutrinos from the gravitational wave event GW150914 possibly associated with a short gamma-ray burst*, *Phys. Rev. D* **93** (2016) 123011 [[arXiv:1602.08436](#)] [[INSPIRE](#)].
- [27] ICECUBE collaboration, M.G. Aartsen et al., *An all-sky search for three flavors of neutrinos from gamma-ray bursts with the IceCube neutrino observatory*, *Astrophys. J.* **824** (2016) 115 [[arXiv:1601.06484](#)] [[INSPIRE](#)].

- [28] P. Padovani, E. Resconi, P. Giommi, B. Arsioli and Y.L. Chang, *Extreme blazars as counterparts of IceCube astrophysical neutrinos*, *Mon. Not. Roy. Astron. Soc.* **457** (2016) 3582 [[arXiv:1601.06550](#)] [[INSPIRE](#)].
- [29] ICECUBE, PIERRE AUGER and TELESCOPE ARRAY collaborations, M.G. Aartsen et al., *Search for correlations between the arrival directions of IceCube neutrino events and ultrahigh-energy cosmic rays detected by the Pierre Auger Observatory and the Telescope Array*, *JCAP* **01** (2016) 037 [[arXiv:1511.09408](#)] [[INSPIRE](#)].
- [30] D. Gaggero, D. Grasso, A. Marinelli, A. Urbano and M. Valli, *The gamma-ray and neutrino sky: a consistent picture of Fermi-LAT, Milagro and IceCube results*, *Astrophys. J.* **815** (2015) L25 [[arXiv:1504.00227](#)] [[INSPIRE](#)].
- [31] C. Lunardini and S. Razzaque, *High energy neutrinos from the Fermi bubbles*, *Phys. Rev. Lett.* **108** (2012) 221102 [[arXiv:1112.4799](#)] [[INSPIRE](#)].
- [32] C. Lunardini, S. Razzaque and L. Yang, *Multimessenger study of the Fermi bubbles: very high energy gamma rays and neutrinos*, *Phys. Rev. D* **92** (2015) 021301 [[arXiv:1504.07033](#)] [[INSPIRE](#)].
- [33] R. Aloisio et al., *Cosmogenic neutrinos and ultra-high energy cosmic ray models*, *JCAP* **10** (2015) 006 [[arXiv:1505.04020](#)] [[INSPIRE](#)].
- [34] K. Murase, R. Laha, S. Ando and M. Ahlers, *Testing the dark matter scenario for PeV neutrinos observed in IceCube*, *Phys. Rev. Lett.* **115** (2015) 071301 [[arXiv:1503.04663](#)] [[INSPIRE](#)].
- [35] K. Murase, D. Guetta and M. Ahlers, *Hidden cosmic-ray accelerators as an origin of TeV–PeV cosmic neutrinos*, *Phys. Rev. Lett.* **116** (2016) 071101 [[arXiv:1509.00805](#)] [[INSPIRE](#)].
- [36] S. Hummer, M. Maltoni, W. Winter and C. Yaguna, *Energy dependent neutrino flavor ratios from cosmic accelerators on the Hillas plot*, *Astropart. Phys.* **34** (2010) 205 [[arXiv:1007.0006](#)] [[INSPIRE](#)].
- [37] S. Hummer, M. Ruger, F. Spanier and W. Winter, *Simplified models for photohadronic interactions in cosmic accelerators*, *Astrophys. J.* **721** (2010) 630 [[arXiv:1002.1310](#)] [[INSPIRE](#)].
- [38] J.G. Learned and S. Pakvasa, *Detecting ν_τ oscillations at PeV energies*, *Astropart. Phys.* **3** (1995) 267 [[hep-ph/9405296](#)] [[INSPIRE](#)].
- [39] J.P. Rachen and P. Meszaros, *Photohadronic neutrinos from transients in astrophysical sources*, *Phys. Rev. D* **58** (1998) 123005 [[astro-ph/9802280](#)] [[INSPIRE](#)].
- [40] T. Kashti and E. Waxman, *Flavoring astrophysical neutrinos: flavor ratios depend on energy*, *Phys. Rev. Lett.* **95** (2005) 181101 [[astro-ph/0507599](#)] [[INSPIRE](#)].
- [41] M. Kachelriess and R. Tomas, *High-energy neutrino yields from astrophysical sources: weakly magnetized sources*, *Phys. Rev. D* **74** (2006) 063009 [[astro-ph/0606406](#)] [[INSPIRE](#)].
- [42] P. Lipari, M. Lusignoli and D. Meloni, *Flavor composition and energy spectrum of astrophysical neutrinos*, *Phys. Rev. D* **75** (2007) 123005 [[arXiv:0704.0718](#)] [[INSPIRE](#)].
- [43] S.R. Klein, R.E. Mikkelsen and J. Becker Tjus, *Muon acceleration in cosmic-ray sources*, *Astrophys. J.* **779** (2013) 106 [[arXiv:1208.2056](#)] [[INSPIRE](#)].
- [44] L.A. Anchordoqui, H. Goldberg, F. Halzen and T.J. Weiler, *Galactic point sources of TeV antineutrinos*, *Phys. Lett. B* **593** (2004) 42 [[astro-ph/0311002](#)] [[INSPIRE](#)].
- [45] J. Bergström, M.C. Gonzalez-Garcia, M. Maltoni and T. Schwetz, *Bayesian global analysis of neutrino oscillation data*, *JHEP* **09** (2015) 200 [[arXiv:1507.04366](#)] [[INSPIRE](#)].
- [46] C.A. Argüelles, T. Katori and J. Salvado, *New physics in astrophysical neutrino flavor*, *Phys. Rev. Lett.* **115** (2015) 161303 [[arXiv:1506.02043](#)] [[INSPIRE](#)].

- [47] H. Athar, C.S. Kim and J. Lee, *The intrinsic and oscillated astrophysical neutrino flavor ratios*, *Mod. Phys. Lett. A* **21** (2006) 1049 [[hep-ph/0505017](#)] [[INSPIRE](#)].
- [48] J.F. Beacom, N.F. Bell, D. Hooper, S. Pakvasa and T.J. Weiler, *Decay of high-energy astrophysical neutrinos*, *Phys. Rev. Lett.* **90** (2003) 181301 [[hep-ph/0211305](#)] [[INSPIRE](#)].
- [49] P. Baerwald, M. Bustamante and W. Winter, *Neutrino decays over cosmological distances and the implications for neutrino telescopes*, *JCAP* **10** (2012) 020 [[arXiv:1208.4600](#)] [[INSPIRE](#)].
- [50] J.F. Beacom et al., *Pseudo-Dirac neutrinos: a challenge for neutrino telescopes*, *Phys. Rev. Lett.* **92** (2004) 011101 [[hep-ph/0307151](#)] [[INSPIRE](#)].
- [51] A. Esmaili, *Pseudo-Dirac neutrino scenario: cosmic neutrinos at neutrino telescopes*, *Phys. Rev. D* **81** (2010) 013006 [[arXiv:0909.5410](#)] [[INSPIRE](#)].
- [52] H. Athar, M. Jezabek and O. Yasuda, *Effects of neutrino mixing on high-energy cosmic neutrino flux*, *Phys. Rev. D* **62** (2000) 103007 [[hep-ph/0005104](#)] [[INSPIRE](#)].
- [53] D. Hooper, D. Morgan and E. Winstanley, *Lorentz and CPT invariance violation in high-energy neutrinos*, *Phys. Rev. D* **72** (2005) 065009 [[hep-ph/0506091](#)] [[INSPIRE](#)].
- [54] L.A. Anchordoqui et al., *Probing Planck scale physics with IceCube*, *Phys. Rev. D* **72** (2005) 065019 [[hep-ph/0506168](#)] [[INSPIRE](#)].
- [55] D. Hooper, D. Morgan and E. Winstanley, *Probing quantum decoherence with high-energy neutrinos*, *Phys. Lett. B* **609** (2005) 206 [[hep-ph/0410094](#)] [[INSPIRE](#)].
- [56] P.F. de Salas, R.A. Lineros and M. Tórtola, *Neutrino propagation in the galactic dark matter halo*, [arXiv:1601.05798](#) [[INSPIRE](#)].
- [57] ICECUBE collaboration, M.G. Aartsen et al., *Flavor ratio of astrophysical neutrinos above 35 TeV in IceCube*, *Phys. Rev. Lett.* **114** (2015) 171102 [[arXiv:1502.03376](#)] [[INSPIRE](#)].
- [58] I.M. Shoemaker and K. Murase, *Probing BSM neutrino physics with flavor and spectral distortions: prospects for future high-energy neutrino telescopes*, *Phys. Rev. D* **93** (2016) 085004 [[arXiv:1512.07228](#)] [[INSPIRE](#)].
- [59] K. Murase and K. Ioka, *TeV–PeV neutrinos from low-power gamma-ray burst jets inside stars*, *Phys. Rev. Lett.* **111** (2013) 121102 [[arXiv:1306.2274](#)] [[INSPIRE](#)].
- [60] K. Murase, Y. Inoue and C.D. Dermer, *Diffuse neutrino intensity from the inner jets of active galactic nuclei: impacts of external photon fields and the blazar sequence*, *Phys. Rev. D* **90** (2014) 023007 [[arXiv:1403.4089](#)] [[INSPIRE](#)].
- [61] V.S. Berezinskii and A.Z. Gazizov, *Cosmic neutrino and the possibility of searching for W bosons with masses 30–100 GeV in underwater experiments*, *JETP Lett.* **25** (1977) 254.
- [62] V. Barger et al., *Glashow resonance as a window into cosmic neutrino sources*, *Phys. Rev. D* **90** (2014) 121301 [[arXiv:1407.3255](#)] [[INSPIRE](#)].
- [63] L.A. Anchordoqui, H. Goldberg, F. Halzen and T.J. Weiler, *Neutrinos as a diagnostic of high energy astrophysical processes*, *Phys. Lett. B* **621** (2005) 18 [[hep-ph/0410003](#)] [[INSPIRE](#)].
- [64] M. Ahlers et al., *Neutrinos as a diagnostic of cosmic ray galactic/extra-galactic transition*, *Phys. Rev. D* **72** (2005) 023001 [[astro-ph/0503229](#)] [[INSPIRE](#)].
- [65] P. Bhattacharjee and N. Gupta, *Probing neutrino mixing angles with ultrahigh energy neutrino telescopes*, [hep-ph/0501191](#) [[INSPIRE](#)].
- [66] S. Pakvasa, W. Rodejohann and T.J. Weiler, *Flavor ratios of astrophysical neutrinos: implications for precision measurements*, *JHEP* **02** (2008) 005 [[arXiv:0711.4517](#)] [[INSPIRE](#)].
- [67] Z.-z. Xing and S. Zhou, *Glashow resonance as a discriminator of ultrahigh-energy cosmic neutrinos originating from $p\gamma$ and pp collisions*, *Phys. Rev. D* **84** (2011) 033006 [[arXiv:1105.4114](#)] [[INSPIRE](#)].

- [68] ICECUBE collaboration, M.G. Aartsen et al., *IceCube-Gen2 — the next generation neutrino observatory at the South Pole. Contributions to ICRC 2015*, [arXiv:1510.05228](#) [INSPIRE].
- [69] KM3NET collaboration, S. Adrián-Martínez et al., *Letter of intent for KM3NeT 2.0*, *J. Phys. G* **43** (2016) 084001 [[arXiv:1601.07459](#)] [INSPIRE].
- [70] PARTICLE DATA GROUP collaboration, K.A. Olive et al., *Review of particle physics*, *Chin. Phys. C* **38** (2014) 090001 [INSPIRE].
- [71] T.S. Sinigovskaya, A.D. Morozova and S.I. Sinigovsky, *High-energy neutrino fluxes and flavor ratio in the Earth's atmosphere*, *Phys. Rev. D* **91** (2015) 063011 [[arXiv:1407.3591](#)] [INSPIRE].
- [72] S. Schonert, T.K. Gaisser, E. Resconi and O. Schulz, *Vetoing atmospheric neutrinos in a high energy neutrino telescope*, *Phys. Rev. D* **79** (2009) 043009 [[arXiv:0812.4308](#)] [INSPIRE].
- [73] T.K. Gaisser, K. Jero, A. Karle and J. van Santen, *Generalized self-veto probability for atmospheric neutrinos*, *Phys. Rev. D* **90** (2014) 023009 [[arXiv:1405.0525](#)] [INSPIRE].